Supporting Information

Kidmose et al. 10.1073/pnas.1003015107

SI Text

Details of Materials and Methods. ***Expression and purification.*** The expression vector pBAD33Ts-Tu-β-3 was kindly provided by Tetsuya Yomo, Osaka University (1). The sequence encoding the tobacco etch virus (TEV) site positioned between the genes encoding EF-Tu and the viral β-subunit was introduced using the Stratagene Quik Change II site-directed mutagenesis kit. Forward and reverse primers had the sequences 5′-GGTGGAGGCGGTGAGAATCTTTATTTTCAGTCAGGCGGAGGTG-3′ and 5′-CACCTCCGCCTGACTGAAAATAAAGATTCTCACCGCCTCCACC-3′, respectively. The resulting plasmid is denoted pBAD33Ts-Tu-TEV-β-3 and the encoded protein is named EF-Ts–EF-Tu–TEV–βS–6xHis. The expression vector pBAD33Ts-Tu-TEV-β-3 was transformed into the *Escherichia coli* strain BL21 (DE3). LB medium containing 34 μg/mL chloramphenicol was inoculated with 1.25% of an overnight culture of the transformed strain. At an OD_{600} of 0.8 the culture grown at 37 °C was induced with 0.2% wt/vol L-arabinose for 3.5 hours. Harvested cells were resuspended in 2 mL lysis buffer (20% glycerol, 0.1 M NaH_2PO_4 pH 8.0, 0.5 M NaCl, 5 mM $MgCl_2$, 1 mM PMSF, 5 mM β-mercaptoethanol, and 0.005% Tween 20) per gram of cells and lysed by sonication followed by ultracentrifugation at $256.000 \times g$ at 4 °C for 75 minutes. The resulting supernatant was filtrated through a 1.0 μm filter and loaded on a 5-mL HIS-trap high performance column (GE Healthcare) equilibrated in His-column buffer A (20% glycerol, 0.1 M Tris-HCl pH 7.6, 0.5 M NaCl, 5 mM $MgCl_2$, 1 mM PMSF, 5 mM β-mercaptoethanol, and 20 mM imidazole). The column was washed in His-column buffer A and bound protein was eluted by a linear gradient of imidazole from 20–250 mM. Relevant fractions were pooled and TEV protease was added, and the sample was left overnight at 4 °C. The TEV-cleaved fusion protein, denoted EF-Ts–EF-Tu:βS–6xHis, was added three volumes of hydrophobic interaction chromatography (HIC)-buffer A (40% $(NH_4)_2SO_4$, 50 mM Tris-HCl pH 7.6, 5 mM $MgCl_2$, 0.5 mM DTT, 1 mM EDTA) and loaded on a 9 mL Source-15 isopropyl column (GE Healthcare) preequilibrated in HIC-buffer A. The column was washed with 25% $(NH_4)_2SO_4$ and eluted by a linear gradient from 25–15% $(NH_4)_2SO_4$. Pooled fractions were loaded on a 120 mL Superdex 200 (GE Healthcare) gel filtration column equilibrated in 0.5 M NaCl, 20 mM Tris-HCl pH 7.8, 1 mM DTT. Peaks corresponding to either monomeric or dimeric EF-Ts–EF-Tu:βS–6xHis with or without bound, endogenous S1 were pooled separately and concentrated to approximately 36 mg/mL as measured by absorption at 280 nm. The molar concentration of the Qβ replicase core preparations was determined by using the value of $A_{0.1\%} = 0.767$, as calculated by ProtParam (http://au.expasy.org/tools/protparam.html).

RNA templates. Poly(C) (Amersham Biosciences) was used for standard Qβ replicase activity assays (2). A previously described 139-nt-long derivative (3) of the minus strand of $RQ135^{-1}$ RNA (4) was used for exploring the ability of Qβ replicase preparations to amplify RNAs and to form replicative complexes.

Gel filtration.
Gel filtration of Qβ replicase preparations was performed using a 1×30 cm Superdex 200 column connected to an AKTAprime plus liquid chromatography system (GE Healthcare), in buffer containing 20 mM Tris-HCl pH 7.5, 1 mM EDTA, 5 mM $MgCl_2$, 5 mM β-mercaptoethanol, and 50 mM or 500 mM NaCl as indicated.

Qβ replicase activity.
Qβ replicase activity was assayed as a poly(C)-directed synthesis of poly(G) (2) at 30 °C (unless otherwise specified) in 10-μL aliquots containing reaction buffer (100 mM Hepes-NaOH pH 7.5, 10 mM $MgCl_2$, 1 mM EDTA), 0.5 μg of a Qβ replicase preparation (which added to the buffer 50 mM NaCl, as well as 1/10 concentration of other components contained in the gel filtration buffer), 0.1 mg/mL poly(C), and 0.2 mM [^{3}H]GTP (25,000 cpm/nmol, Amersham Biosciences). Where indicated, pentaerythritol propoxylate (5/4 PO/OH) (PEP) was also present at the specified concentration. After incubation for 1 min (during which the reaction kinetics remained linear), the reaction was terminated by adding 5 μL of 30 mM EDTA and transferring the test tube on ice. The sample was then applied to a 1×1 cm piece of Hybond N nylon membrane (Amersham Biosciences). The membrane was dried, washed 3 times for 3 min in a cold (4 °C) solution containing 3% H_3PO_4, 20 mM $Na_2P_2O_7$, 1 mM EDTA, and once for 3 min in cold 75% ethanol (1 mL of a solution was used per membrane). After drying, the membrane was placed in 2.5 mL of a scintillation cocktail [0.02% 1,4-bis(5-phenyl-2-oxazolyl)benzene, 0.4% 2,5-dephenyloxazole in toluene], and its radioactivity was determined using a Beckman LS 6500 counter. Specific activity of the enzyme was expressed in nmoles of GMP incorporated for 10 min at 30 °C into the acid-insoluble material [the unit definition of Qβ replicase (2)] per 1 mg of protein.

Temperature inactivation.
Temperature inactivation of the Qβ replicase preparations was performed in 8 μL of the $1.25 \times$ reaction buffer (125 mM Hepes-NaOH pH 7.5, 12.5 mM $MgCl_2$, 1.25 mM EDTA) containing 0.5 μg of the enzyme during 10 min at the indicated temperature, followed by 30 s at 30 °C. Thereafter each sample was mixed with 2 μL of a solution containing poly(C) and [^{3}H]GTP to a final concentration of 0.1 mg/mL and 0.2 mM, respectively, and the residual Qβ replicase activity was assayed as above.

RNA amplification.
RNA amplification was carried out at 30 °C in the reaction buffer (see above) containing 1 mM each of ATP, CTP, and GTP, 1 mM [α-^{32}P]UTP (1 MBq/μmol, Institute of Bioorganic Chemistry), 0.5 nM RQ135 RNA, and 100 nM monomer equivalent of a Qβ replicase preparation. At the indicated time points, 10-μL aliquots were withdrawn, mixed with 5 μL of 30 mM EDTA, and placed on ice. Each sample was extracted with 15 μL of phenol/chloroform (1:1, vol/vol), and 10 μL of the aqueous phase was subjected to nondenaturing PAGE (3). After silver staining (5), the gels were dried on a filter paper. The ^{32}P-labeled RNA bands were revealed using a Cyclone™ phosphor storage system (Packard Instrument) and quantified by measuring the band intensity on 16-bit TIFF images using the OptiQuant™ Image Analysis Software (Packard Instrument).

Formation of replicative complexes.
Formation of replicative complexes was detected by a gel shift assay. One pmol of monomer equivalent of the monomer or dimer was incubated at 22 °C for 10 min with 0.25 pmol of RQ135 RNA (premelted in 1 mM EDTA) in 10 μL of the reaction buffer (see above) containing 1 mM GTP and, where indicated, 10 μM CTP and 3 μM [α-^{32}P]UTP, with or without 10 μM ATP. Specific activity of [α-^{32}P]UTP was 0.3 MBq/nmol in the reactions without ATP and 0.01 MBq/nmol in the reactions with ATP. The concentration of UTP (3 μM) allowed only a few replication

rounds to occur and to keep the molar amount of RNA product lower than the amount of enzyme. After the addition of 1 μL of the sample buffer (50% glycerol, 0.05% bromophenol blue, 0.05% xylenecyanol, 1 mM EDTA) and chilling on ice for 20 min, the samples were subjected to nondenaturing electrophoresis through a 8% polyacrylamide gel during 2 h at 10–12 °C in buffer TBE (89 mM Tris base, 89 mM boric acid, 2 mM EDTA) containing 10% glycerol and 3 mM $MgCl_2$. The gel was stained with silver (5) and dried, and ^{32}P-labeled bands were revealed as above.

Structure determination. Plate-shaped crystals were grown by vapor diffusion in sitting drops at 4 °C with a reservoir buffer containing 0.2 M KCl, 0.05 M Hepes-NaOH pH 7.5, and 27–30% vol/vol PEP. The protein sample consisted of 1 μL EF-Ts–EF-Tu · βS–6xHis (36 mg/mL) added a two molar surplus of guanosine-5′-[(β,γ)-imido]triphosphate (GDPNP) and was mixed with 1 μL of reservoir buffer. Crystals were soaked prior to flash freezing in a buffer containing 0.2 M KCl, 0.05 M Hepes-NaOH pH 7.5, and 35% PEP. Diffraction data were collected at the European Synchrotron Radiation Facility (Table S1) and processed with XDS (6). Initial model phases were obtained by using the structure (Research Collaboratory for Structural Bioinformatics entry 1EFU) of the EF-Tu:EF-Ts complex (coiled-coil motif of EF-Ts removed) as search model in molecular replacement with the program PHASER (7), which identified two copies of the search model. An improved electron density was obtained by density modification with CNS (8), and the resulting phases were input to RESOLVE (9), which located significant parts for the replicase subunits. From this point, the model was improved in an iterative manner by phase calculation, density modification, and rebuilding. Upon convergence of this cycle, one copy of the Qβ core replicase was rebuild manually with COOT (10) in a twofold averaged electron density map where after the second copy was generated by the noncrystallographic symmetry operator. A second iterative cycle consisting of model refinement with PHENIX.REFINE (11) followed by manual rebuilding was carried out until convergence. Noncrystallographic symmetry restraints were used throughout all refinement with EF-Tu divided into two bodies, EF-Ts was used as one body, and the β-subunit divided into three bodies. In the final structure, 1,192 C^{α} atoms from the one core replicase monomer superimpose onto the second core replicase with an rmsd of 0.28 Å, indicating very small structural differences between these. Crystallization required the presence of the nonhydrolyzable GTP analog, GDPNP, but the nucleotide could not be found in the electron density regardless of whether 5 mM Mg^{2+} was present or not during crystallization and cryoprotection. In the final cycles, the model was validated with MOLPROBITY (12) and PROCHECK (13). Ramachandran plot statistics were calculated with the latter program. Figures were prepared with PYMOL (14) or ALINE (15) and conformational changes analyzed with DYNDOM (16). The electrostatic potential was plotted on the solvent accessible surface with the APBS (17) plug-in for PYMOL. Charge and radius parameters according to an AMBER force field were assigned to the Protein Data Bank (PDB) file by the PDB2PQR Web server (18). Homology searches were conducted with DALI (19).

1. Kita H, et al. (2006) Functional Qβ replicase genetically fusing essential subunits EF-Ts and EF-Tu with beta-subunit. *J Biosci Bioeng* 101:421–426.
2. Kamen R (1972) A new method for the purification of Qβ RNA-dependent RNA polymerase. *Biochim Biophys Acta* 262:88–100.
3. Ugarov VI, Demidenko AA, Chetverin AB (2003) Qβ replicase discriminates between legitimate and illegitimate templates by having different mechanisms of initiation. *J Biol Chem* 278:44139–44146.
4. Munishkin AV, et al. (1991) Efficient templates for Qβ replicase are formed by recombination from heterologous sequences. *J Mol Biol* 221:463–472.
5. Igloi GL (1983) A silver stain for the detection of nanogram amounts of tRNA following two-dimensional electrophoresis. *Anal Biochem* 134:184–188.
6. Kabsch W (2001) XDS. *International Tables for Crystallography*, eds Rossmann MG, Arnold E (Kluwer Academic, Dordrecht), Vol F.
7. McCoy AJ (2007) Solving structures of protein complexes by molecular replacement with Phaser. *Acta Crystallogr D* 63:32–41.
8. Brunger AT, et al. (1998) Crystallography & NMR system: A new software suite for macromolecular structure determination. *Acta Crystallogr D* 54:905–921.
9. Terwilliger TC (2003) Automated main-chain model building by template matching and iterative fragment extension. *Acta Crystallogr D* 59(Pt 1):38–44.
10. Emsley P, Cowtan K (2004) Coot: Model-building tools for molecular graphics. *Acta Crystallogr D* 60:2126–2132.
11. Adams PD, et al. (2002) PHENIX: Building new software for automated crystallographic structure determination. *Acta Crystallogr D* 58:1948–1954.
12. Lovell SC, et al. (2003) Structure validation by Cα geometry: Phi, psi and Cβ deviation. *Proteins* 50:437–450.
13. Laskowski RA, MacArthur MW, Moss D, Thornton JM (1993) PROCHECK: A program to check the stereochemical quality of protein structures. *J Appl Crystallogr* 26:283–291.
14. DeLano WL (2002) *The PyMOL User's Manual* (DeLano Scientific, San Carlos, CA).
15. Bond CS, Schuttelkopf AW (2009) ALINE: A WYSIWYG protein sequence alignment editor for publication quality alignments. *Acta Crystallogr D* 65:510–512.
16. Hayward S, Berendsen HJ (1998) Systematic analysis of domain motions in proteins from conformational change: New results on citrate synthase and T4 lysozyme. *Proteins* 30:144–154.
17. Baker NA, Sept D, Joseph S, Holst MJ, McCammon JA (2001) Electrostatics of nanosystems: Application to microtubules and the ribosome. *Proc Natl Acad Sci USA* 98:10037–10041.
18. Dolinsky TJ, Nielsen JE, McCammon JA, Baker NA (2004) PDB2PQR: An automated pipeline for the setup of Poisson-Boltzmann electrostatics calculations. *Nucleic Acids Res* 32:W665–667.
19. Holm L, Kaariainen S, Rosenstrom P, Schenkel A (2008) Searching protein structure databases with DaliLite v.3. *Bioinformatics* 24:2780–2781.

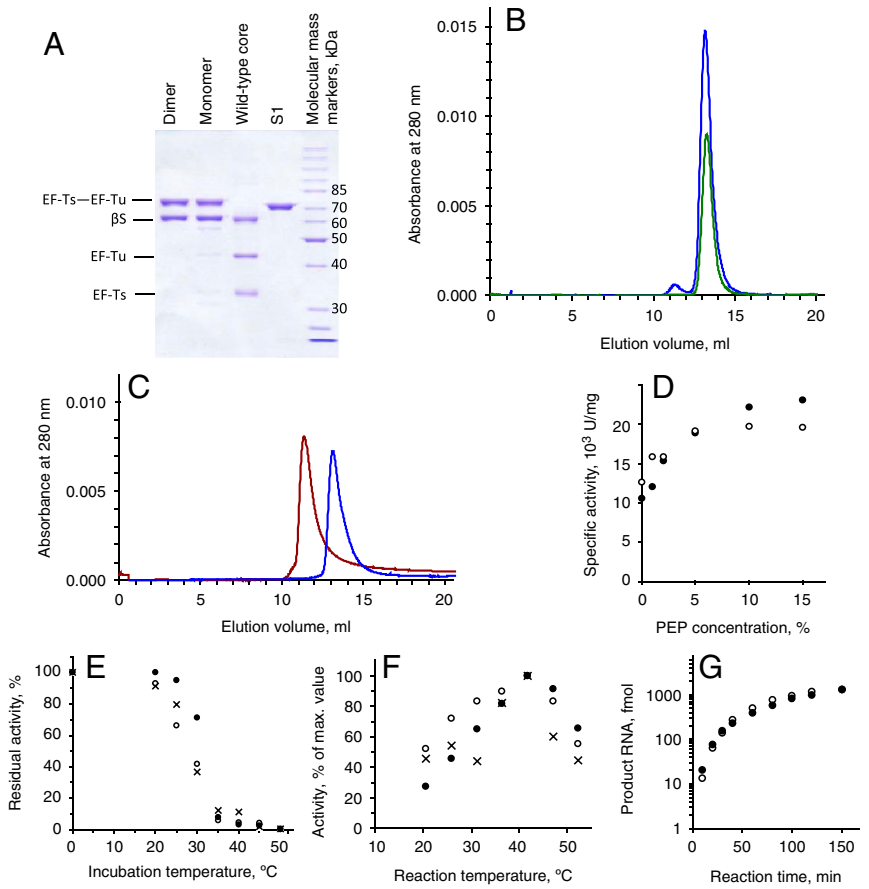

Fig. S1. Characterization of the Qβ replicase preparation used for structure determination. (*A*) SDS-PAGE analysis. The gel was stained with Coomassie blue R-250. βS denotes the β-subunit. (*B*) Gel filtration of the isolated monomer (*Blue*) and of the wild-type Qβ replicase core complex (*Green*) in a buffer containing 500 mM NaCl. The presence of a small amount of the dimer in the monomer preparation seems to be due to incomplete separation of the two forms during the isolation the monomer. (*C*) Gel filtration of the isolated dimer (*Red*) and monomer (*Blue*) in a buffer containing 50 mM NaCl. The wide asymmetric form of the peaks seems to be due to dissociation of the Qβ replicase core into the viral β subunit and the EF-Ts–EF-Tu fusion protein in the low salt buffer. (*D*) Effects of increasing concentrations of PEP in the poly(C) assay buffer on the specific activity. Open circles, filled circles, and crosses symbolize the monomer, the dimer, and the wild-type core enzyme, respectively, in this and the following panels. (*E*) Activity loss upon incubation in a low salt buffer during 10 min at the indicated temperatures. (*F*) Temperature dependence of the poly(C)-directed activities of the monomer, dimer, and the wild-type Qβ replicase core. (*G*) Time course of the amplification of 5 fmol RQ135 RNA by 1,000 fmol of the monomer or 500 fmol of the dimer at 30 °C. The semilogarithmic plot allows the exponential and linear amplification phases to be distinguished. For further details, see *Details of Materials and Methods*.

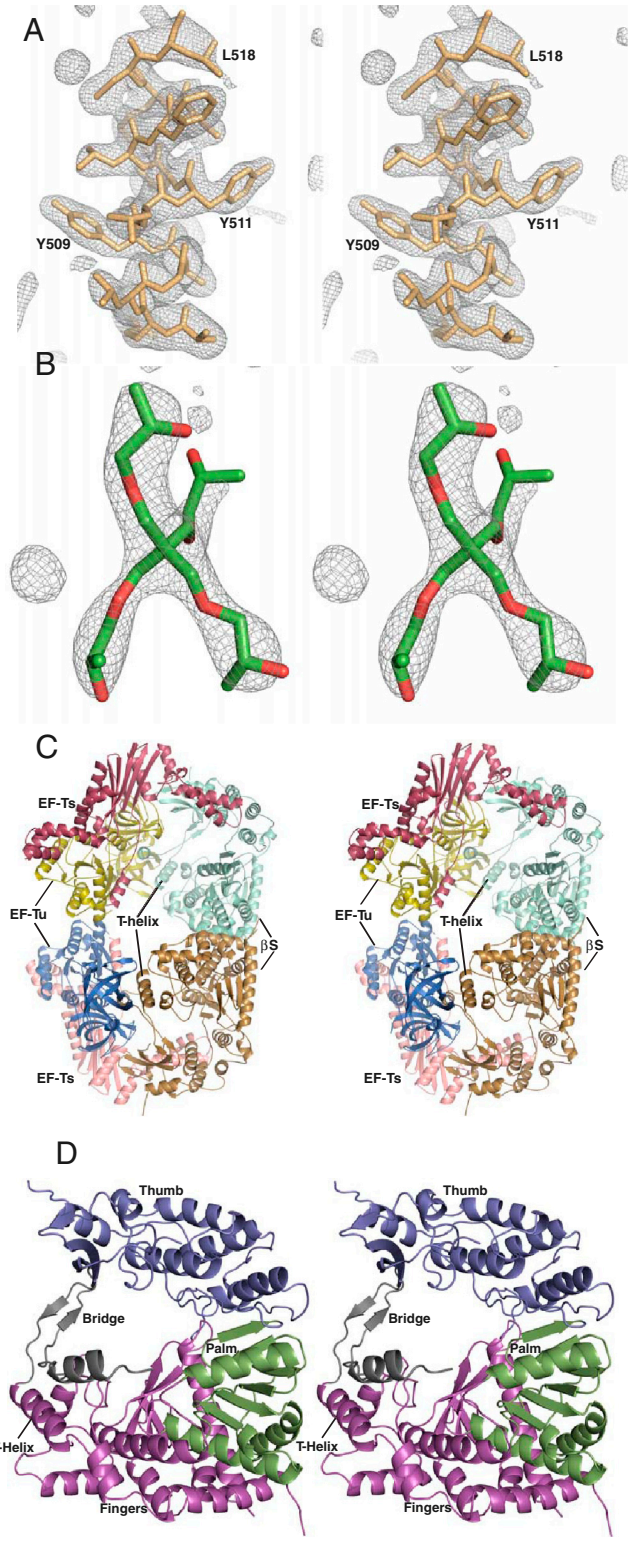

Fig. S2. Structure determination of the dimeric Qβ core replicase. (*A*) Stereo view of an omit mF_o-DF_c electron density map contoured at 3.0σ around the T helix of the β-subunit. (*B*) Stereo view of an omit mF_o-DF_c electron density map contoured at 3.0σ around the PEP bound between the β-subunit and EF-Tu. (*C*) Stereo view of a cartoon representation of the dimeric replicase found in the asymmetric unit of the crystal. The two monomers are related by a horizontal twofold rotation axis. (*D*) Stereo view of a cartoon representation of the β-subunit shown in the same orientation as in Fig. 2*B*.

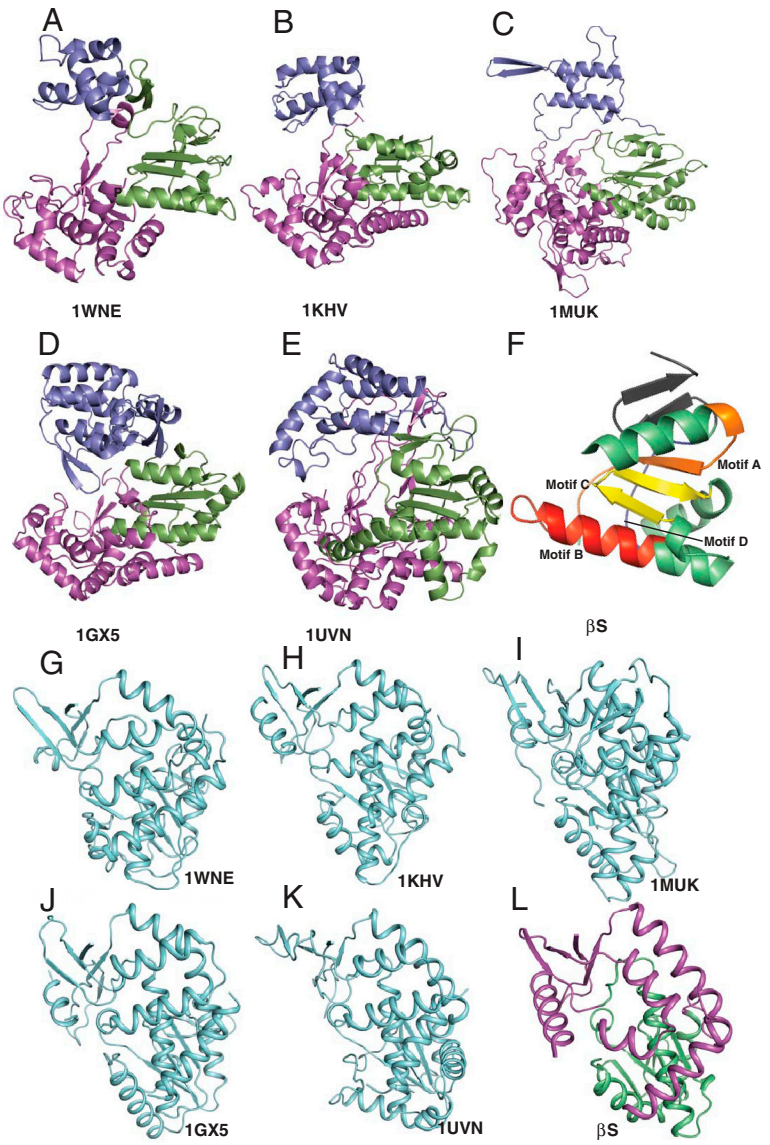

Fig. S3. Cartoon representation of five RNA-dependent RNA polymerases (*A–E*) in the same orientation and color as in Fig. 2*B* and of a recurring structural entity identified in all six RdRps comprised of the palm and a subdomain of the fingers domain (*G–L*). (*A* and *G*) Foot and mouth disease virus RNA-dependent RNA polymerase (PDB ID code 1WNE). (*B* and *H*) Rabbit hemorrhagic disease virus RNA-dependent RNA polymerase (PDB ID code 1KHV). (*C* and *I*) Reovirus polymerase λ3 (PDB ID code 1MUK). (*D* and *J*) Hepatitis C virus RNA polymerase (PDB ID code 1GX5). (*E* and *K*) RNA-dependent RNA polymerase phi6p2 (PDB ID code 1UVN). (*F*) Cartoon representation of the palm domain of the β-subunit displaying motifs *A–D*. (*L*) The conserved recurring structural entity from the β-subunit colored by domains (fingers magenta and palm green). Subjection of this entity to a DALI search retrieves the Hepatitis C virus RdRp (PDB ID code 3I5 K) with a *Z* score of 8.7 and a rmsd of 3.4 Å over 230 superimposed C^{α} atoms compared to 251 residues from the β-subunit in this entity.

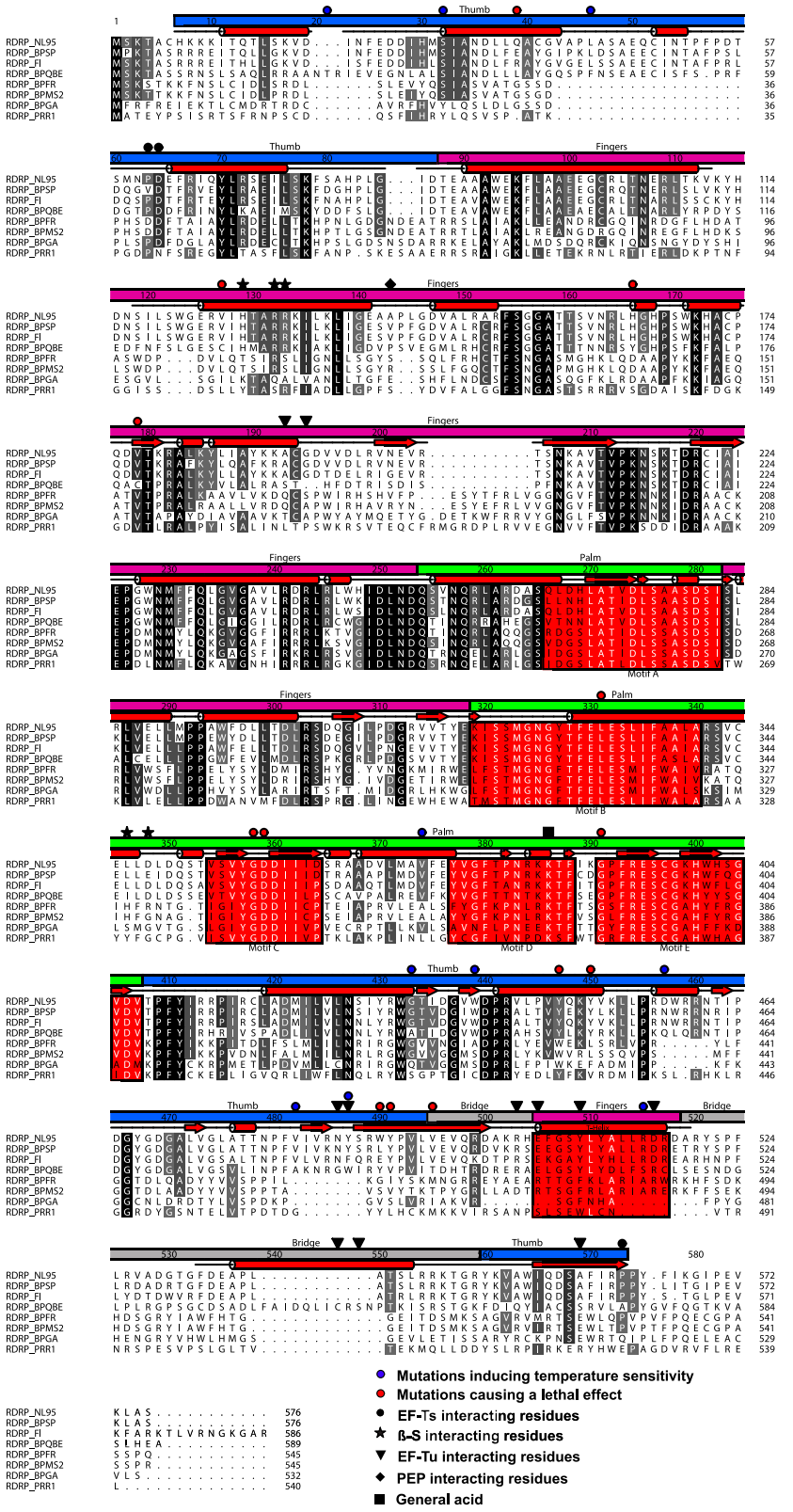

Fig. S4. Alignment of RdRp sequences from the virus family *Leviviridae*. The enterobacteriophages (BP) NL95, SP, FI, and Qβ (QBE) belong to the *Allolevirus* genus, the enterobacteriophages FR, MS2, and GA belongs to the *Levivirus* genus, and PRR1 is a pseudomonas phage figuring as an unclassified *Leviviridae* virus. Inspection of the alignment combined with the new structural knowledge suggests that PRR1 should be classified as a *Levivirus*. Lethal mutations in the β-subunit (Table S2) and mutations inducing temperature sensitivity are marked with red and blue spheres, respectively.

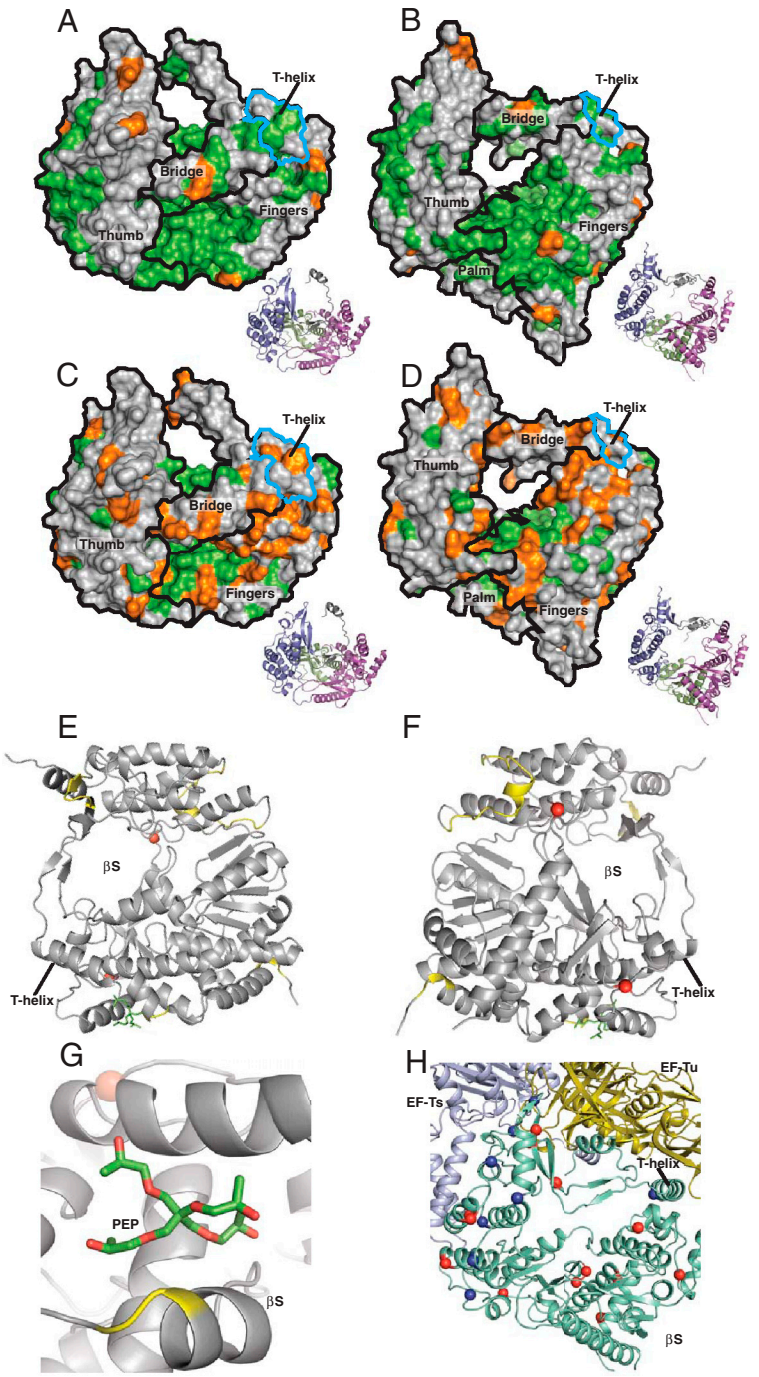

Fig. S5. Comparison of the RdRps from *Allolevirus* and *Levivirus*. (*A* and *B*) Surface representation of the β-subunit (two different orientations; *A* has the same orientation as in Fig. 4*C*) colored according to conservation among *Allolevirus* RdRps in the sequence alignment shown in Fig. S4. Strictly conserved residues are colored green, highly conserved residues are colored orange, and nonconserved residues are colored gray. Small cartoon thumbnails with domains colored as in Fig. 2*B* are shown for comparison. The location of the palm, fingers, and thumb domains are indicated with black outlines on the surface, whereas the T helix is indicated with a blue outline. (*C* and *D*) As in *A* and *B*, but colored after conservation among *Levivirus* RdRps. (*E* and *F*) Cartoon representation of the β-subunit displaying inserts (*Yellow*) and deletions (*Red Spheres*) present in *Allolevivirus* relative to *Levivirus* shown in two different orientations. (*G*) Close-up of the PEP binding site displaying the existence of an insert present right at the PEP binding pocket (*Yellow Highlight*). (*H*) Cartoon representation of the Qβ replicase monomer displaying the location of the known mutations of the β-subunit as listed in Table S2. Only mutations causing a lethal effect (*Red Spheres*) and mutations inducing temperature sensitivity (*Blue Spheres*) are indicated.

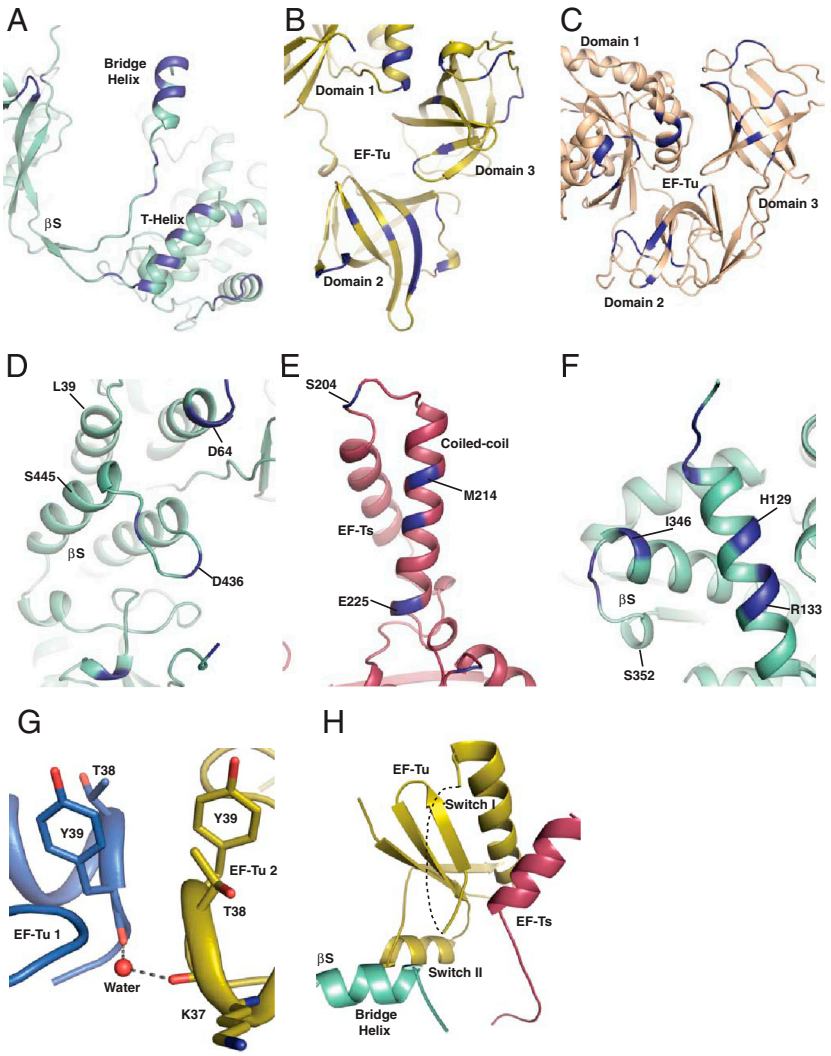

Fig. S6. Interactions between the subunits of the dimeric core replicase. (*A*) EF-Tu footprint onto the β-subunit. Residues in the viral subunit colored blue have atoms within 3.8 Å of atoms in EF-Tu. (*B*) Footprint (*Blue Residues*) of the β-subunit onto EF-Tu. *B* is related to *A* by a vertical rotation of 180°. (*C*) Footprint (*Blue Residues*) of aa-tRNA onto EF-Tu:GTP for comparison with *B*. The orientation is changed relative to *B* to visualize aa-tRNA interactions with EF-Tu domain 1. (*D*) Footprint (*Blue Residues*) of EF-Ts onto the β-subunit. (*E*) Footprint (*Blue Residues*) of the β-subunit onto EF-Ts. *E* is related to *D* by a vertical rotation of 180°. (*F*) Footprint of the β-subunit dimerization interface. Interacting surfaces are highlighted in blue. (*G*) Detailed view of the EF-Tu:EF-Tu dimerization interface. A water molecule links the two EF-Tu molecules; otherwise, only van der Waals interactions are present at this interface. (*H*) Close-up of the bridge helix from the β-subunit located near the switch I (disordered, represented by a dashed line) and switch II regions of EF-Tu.

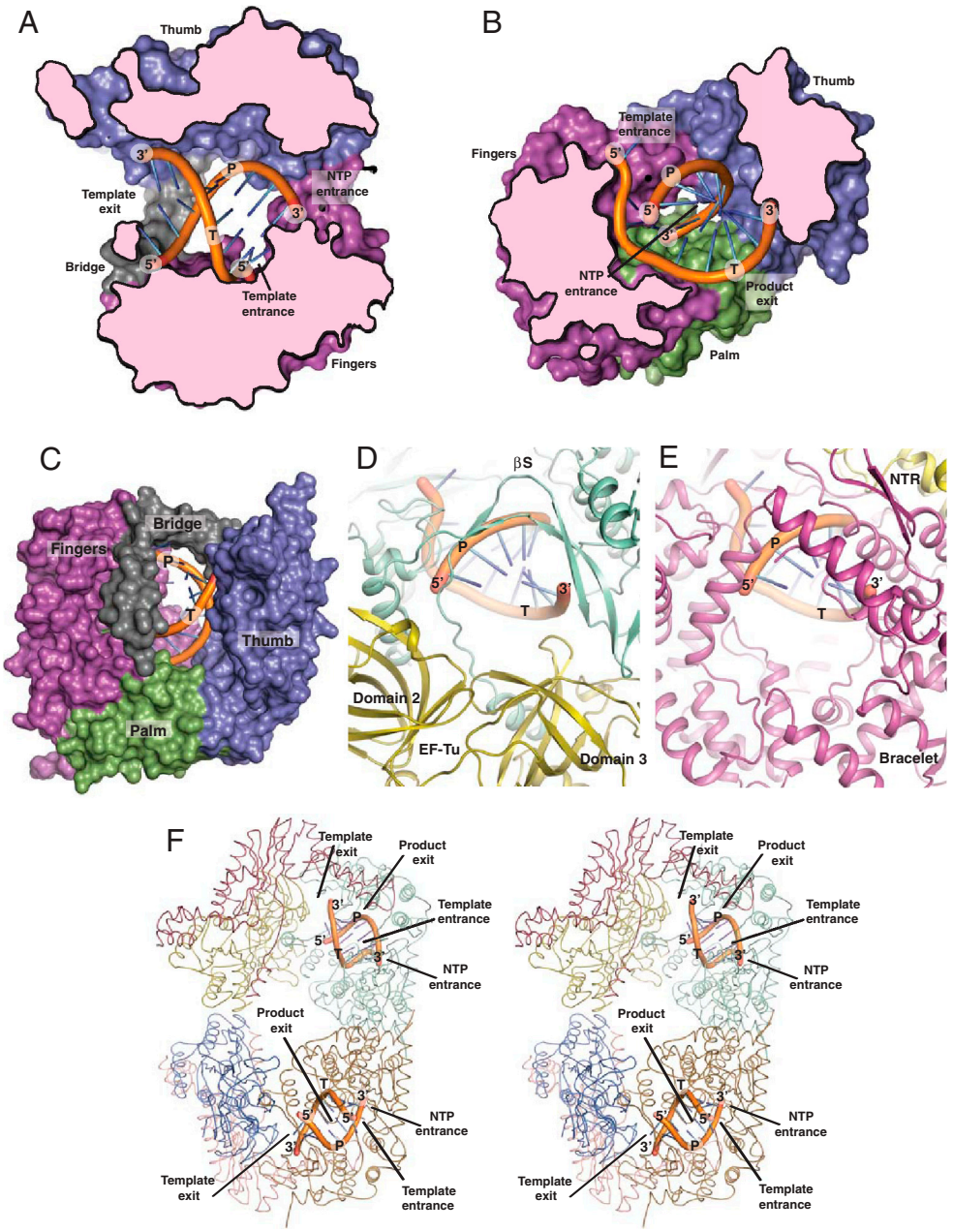

Fig. S7. The putative entrance and exit channels. The double-stranded RNA was docked by comparison with the structure of the Norwalk virus RdRp (PDB ID code 3BSN). Labels "P" and "T" on the RNA backbones denote product and template strand, respectively. The 3′ and 5′ ends of product and template are also indicated. (*A*) View from the palm domain displaying both the suggested entrance and exit channels for the template together with the NTP entrance channel. (*B*) View down from the bridge region displaying both the template and NTP entrance channels and the suggested product exit channel. (*C*) Surface representation of the β-subunit displaying the four domains relative to the docked RNA model as seen from the outside. (*D*) The annular motif in the Qβ replicase is comprised of the bridge region from the β-subunit (*Green*) and of domain 2 and 3 from EF-Tu (*Yellow*). (*E*) The annular motif in the λ3 RdRp (PDB ID code 1MUK) is solely comprised of a C-terminal domain termed the bracelet. The RNA shown in both panels is from the Norwalk virus RdRp docked onto the β-subunit. The λ3 RdRp was superimposed onto the β-subunit by matching conserved secondary structure in the palm domain. (*F*) Stereo view of the core replicase dimer with a docked template-product duplex showing the relationship between the entry/exit sites in the dimer.

Table S1. Statistics for data collection and refinement

Data collection	
Beam line	European Synchrotron Radiation Facility ID14-1
Space group	C2
Unit-cell parameters	$a = 245.76$ Å, $b = 139.47$ Å, $c = 101.596$, $\beta = 92.15°$
Unique reflections	122,562
Resolution (Å)	47.3–2.5 (2.6–2.5)
Redundancy	3.8 (3.8)
Completeness (%)	99.9 (99.9)
Mean I/σ	18.29 (2.87)
R_{sym} (%)	11.2 (57.1)
Refinement	
Resolution (Å)	47.3–2.5
R factor/R_{free} factor (%)	21.0/23.0
Reflections (work/test)	120,569/1,993
Number of atoms in asymmetric unit	Protein 18446/PEP 50/Water 966
rmsd bonds (Å)/angles (°)/B factor (Å^2)	0.008/1.108/3.8
Ramachandran plot (%)	Most favored 92.9, additionally allowed 6.8, generously allowed 0.1, disallowed 0.2
Average B factor (Å^2)	EF-Tu:54 , EF-Ts:80 , β-subunit:43, water 50

$R_{sym} = (\Sigma_h \Sigma_i |I(h)_i - \langle I(h) \rangle| / \Sigma_h \Sigma_i I(h)_i)$ for the intensity of reflection h measured N times. Values in brackets are for outer resolution shell. R factor $= (\Sigma_h ||F_o| - k|F_c|| / \Sigma_h |F_o|)$, where F_o and F_c are the observed and calculated structure factor, respectively, and k is a scaling factor. R_{free} factor is identical to the R factor on a subset of test reflections not used in refinement.

Table S2. Known effects of mutations in the Qβ replicase subunits when part of the Qβ replicase complex

Subunit	Mutation	Phenotype	Reference
β-subunit (588 aa)	C-terminal deletions up to position 571	Dispensable for replicase activity in vitro and phage propagation.	(1)
	C-terminal deletions up to positions 565–570	Replicase activity increased in vitro, relaxed template specificity. Decreased phage propagation ability.	
	C-terminal deletions up to positions 512–564	D	
	S7-grss-R8	WT	(2); replicase activity tested in vivo
	T21-edrss-R22	WT at 30 °C, TS at 42 °C	
	G27-nedlr-N28	WT	
	L31-grss-I33	WT at 30 °C, TS at 42 °C	
	L39-gkifp-A40	D	
	P45-ledrss-N47	WT at 30 °C, TS at 42 °C	
	G61-tedlp-T62	WT	
	R112-grss-P113	WT	
	P113-edrss-Y114	WT	
	C127-1-stop-r-H129	D	
	S165-wkifh-G167	D	
	C179-grss-T180	D	
	L331-drsv-E332	D	
	E373-fl-F375	WT at 30 °C, TS at 42 °C	
	G391-grss-P392	D	
	W432-gkifp-T434	WT at 30 °C, TS at 42 °C	
	W439-dpdl-D440	WT at 30 °C, TS at 42 °C	
	V446-wkifh-L448	D	
	Y450-grsif-R451	D	
	Q457-hrss-L458	WT at 30 °C, TS at 42 °C	
	F481-gkifp-K483	WT at 30 °C, TS at 42 °C	
	W487-iqiw-I488	WT at 30 °C, TS at 42 °C	
	R489-wkifh-V491	D	
	V491-edlp-P492	D	
	T495-dgrss-T496	D	
	S515-grss-R516	WT	
	S515-grsif-R516	WT at 30 °C, TS at 42 °C	
	G357A/P/M/S/V	In vitro activities ≤5% of WT; rescued by Mn^{2+}; D in vivo; phage infection repressed	(3, 4)
	D358S	D	(4)
	D359V	D	
	G390A	Phage growth reduced by 50%	(3)
EF-Tu (398 aa)	R58E reduced binding of aa-tRNA (5)	50% of WT	(6); replicase activity tested on purified complexes
	E259YE 259 binds CCA-3′-aa end of aa-tRNA detective in aa-tRNA binding (7)	D	
	R288E R288 binds the 5′ end of tRNA; R58E shows reduced binding of aa-tRNA (8)	D	
	A375T Kirromycin resistant	5–10% of WT activity in poly(C) replication; rescued by replacement of Mg with Mn; 50% of WT activity in replicating Qß RNA	(9)
EF-Ts (283 aa)	D184-epggea-E225 coiled-coil deleted	Mutant strain resistant towards bacteriophage Qß infection.	(10)

Single amino acid codes are used to indicate the position of mutations. Insertions are indicated by lowercase letters. WT, wild-type; D, dead (≤1% of WT activity); TS, temperature sensitive

1 Inokuchi Y, Kajitani M (1997) Deletion analysis of Qβ replicase. Participation of the carboxyl-terminal region of the beta-subunit protein in template recognition. *J Biol Chem* 272:15339–15345.
2 Mills DR, Priano C, DiMauro P, Binderow BD (1989) Qβ replicase: Mapping the functional domains of an RNA-dependent RNA polymerase. *J Mol Biol* 205:751–764.
3 Inokuchi Y, Hirashima A (1987) Interference with viral infection by defective RNA replicase. *J Virol* 61:3946–3949.
4 Inokuchi Y, Kajitani M, Hirashima A (1994) A study on the function of the glycine residue in the YGDD motif of the RNA-dependent RNA polymerase β-subunit from RNA coliphage Qβ. *J Biochem* 116:1275–1280.
5 Knudsen CR, Clark BF (1995) Site-directed mutagenesis of Arg58 and Asp86 of elongation factor Tu from *E. coli*: effects on the GTPase reaction and aminoacyl-tRNA binding. *Prot Eng* 8:1267–1273.
6 Mathu SGJ, Knudsen CR, van Duin J, Kraal B (2003) Isolation of Qβ polymerase complexes containing mutant species of elongation factor Tu. *J Chromatogr B* 786:279–286.
7 Pedersen GN, Rattenborg T, Knudsen CR, Clark BFC (1988) The role of Glu259 in Escherichia coli elongation factor Tu in ternary complex formation. *Prot Eng* 11:101–108.
8 Rattenborg T, Pedersen GN, Clark BFC, Knudsen CR (1997) Contribution of Arg288 of Escherichia coli elongation factor Tu to translation functionality. *Eur J Biochem* 249:408–414.
9 Blumenthal T, Saari B, Van der Meide PH, Bosch L (1980) Qβ replicase containing wild type and mutant tufA and tufB gene products. *J Biol Chem* 255:5300–5305.
10 Karring H, et al. (2004) Qβ-phage resistance by deletion of the coiled-coil motif in elongation factor Ts. *J Biol Chem* 279:1878–1884.

Table S3. Comparison of molecular interfaces calculated by PISA (1)

Interface	Buried surface area (Å^2)	Δ^iG (kcal/mol)*	Δ^iG *P*-value†
β-subunit: β-subunit	1,770	−9.0	0.305
β-subunit:EF-Tu	3,766	−22.9	0.040
β-subunit:EF-Ts	1,522	−12.1	0.109
EF-Tu:EF-Tu	556	−0.7	0.386

*Solvation free energy gain upon formation of the interface. This does not include salt bridges and hydrogen bonds.

†Probability of getting a lower than obtained Δ^iG, if interface atoms are picked randomly from protein surface such as to amount to the observed interface area. *P* value is a measure of interface specificity, showing how surprising, in energy terms, the interface is. A value of $P = 0.5$ indicates an average hydrophobicity of the interface, at $P > 0.5$ the interface is less hydrophobic than could be expected, and at $P < 0.5$ the interface is more hydrophobic than could be expected.

1 Krissinel E, Henrick K (2007) Inference of macromolecular assemblies from crystalline state. *J Mol Biol* 372:774–797.